Harmonic disturbance observer-based sliding mode control of MEMS gyroscopes

Rui ZHANG[1,2], Bin XU[1,2*], Qi WEI[3], Pengchao ZHANG[4] & Ting YANG[1,2]

[1]*Research and Development Institute of Northwestern Polytechnical University in Shenzhen, Shenzhen 518057, China;*
[2]*School of Automation, Northwestern Polytechnical University, Xi'an 710072, China;*
[3]*Department of Precision Instruments, Tsinghua University, Beijing 100084, China;*
[4]*Shaanxi Provincial Key Laboratory of Industrial Automation, Shaanxi University of Technology, Hanzhong 723000, China*

Citation Zhang R, Xu B, Wei Q, et al. Harmonic disturbance observer-based sliding mode control of MEMS gyroscopes. Sci China Inf Sci, 2022, 65(3): 139201, https://doi.org/10.1007/s11432-019-2841-9

Dear editor,

For micromechanical (MEMS) gyroscopes, the control performance is significantly reduced by the parameter uncertainties and the external disturbances. In view of the parameter perturbations, the adaptive algorithm [1] is first applied to gyroscope control. Then neural networks [2] and fuzzy logic systems [3] are utilized to relax the requirement of precise mathematical models. For the external disturbances, the active disturbance rejection control forces the drive axis to resonate with a fixed amplitude. More studies [4] focus on the disturbance observer (DOB) to achieve better tracking performance. In recent years, the extended state observer (ESO) [5] is integrated with DOB to obtain better performance. Owing to the insensitivity of environmental changes and external disturbances, the sliding mode control (SMC) [2,6] is employed to improve the robustness of MEMS gyroscopes. However, most DOB-based controllers focus on the system stability while ignoring the specific characteristics of the disturbances.

For the external disturbances with harmonic characteristics, the harmonic disturbance observer (HDOB)-based SMC is proposed in this study to control the dynamics of MEMS gyroscopes. By fully using the frequency information of harmonic disturbances, higher tracking accuracy is obtained. Furthermore, the global fast terminal (GFT) SMC, known as GFTSMC, is integrated with HDOB to achieve finite-time convergence.

MEMS gyroscope dynamics. From [7], considering the parameter perturbations and the external disturbances, the dimensionless dynamics of MEMS gyroscopes is presented as follows:

$$\ddot{\boldsymbol{\vartheta}} = \boldsymbol{K}_1^0 \dot{\boldsymbol{\vartheta}} + \boldsymbol{K}_2^0 \boldsymbol{\vartheta} + \boldsymbol{\mu} + \boldsymbol{K}_3 \boldsymbol{\vartheta}^3 + \boldsymbol{K}_d \boldsymbol{D} + \boldsymbol{U}, \qquad (1)$$

where

$$\boldsymbol{K}_1^0 = \begin{bmatrix} -\dfrac{c_{11}^0}{m\omega_o} & \dfrac{2\Omega_z^*}{\omega_o} - \dfrac{c_{12}^0}{m\omega_o} \\ -\dfrac{2\Omega_z^*}{\omega_o} - \dfrac{c_{21}^0}{m\omega_o} & -\dfrac{c_{22}^0}{m\omega_o} \end{bmatrix},$$

$$\boldsymbol{K}_2^0 = \begin{bmatrix} \dfrac{\Omega_z^{*2}}{\omega_o^2} - \dfrac{k_{11}^0}{m\omega_o^2} & -\dfrac{k_{12}^0}{m\omega_o^2} \\ -\dfrac{k_{21}^0}{m\omega_o^2} & \dfrac{\Omega_z^{*2}}{\omega_o^2} - \dfrac{k_{22}^0}{m\omega_o^2} \end{bmatrix}, \quad \boldsymbol{\vartheta} = \begin{bmatrix} \dfrac{\vartheta_1^*}{\vartheta_0} \\ \dfrac{\vartheta_2^*}{\vartheta_0} \end{bmatrix},$$

$$\boldsymbol{\mu} = \Delta \boldsymbol{K}_1 \dot{\boldsymbol{\vartheta}} + \Delta \boldsymbol{K}_2 \boldsymbol{\vartheta},$$

$$\boldsymbol{K}_3 = \begin{bmatrix} -\dfrac{k_{13}\vartheta_o^2}{m\omega_o^2} & 0 \\ 0 & -\dfrac{k_{23}\vartheta_o^2}{m\omega_o^2} \end{bmatrix}, \quad \boldsymbol{K}_d = \begin{bmatrix} k_{d1} & 0 \\ 0 & k_{d2} \end{bmatrix},$$

$$\boldsymbol{D} = \begin{bmatrix} -\dfrac{d_1^*(t^*)}{m\omega_o^2 \vartheta_o} \\ -\dfrac{d_2^*(t^*)}{m\omega_o^2 \vartheta_o} \end{bmatrix}, \quad \boldsymbol{U} = \begin{bmatrix} \dfrac{u_1^*}{m\omega_o^2 \vartheta_o} \\ \dfrac{u_2^*}{m\omega_o^2 \vartheta_o} \end{bmatrix},$$

with the mass m, the position ϑ_i^*, the speed $\dot{\vartheta}_i^*$, and the acceleration $\ddot{\vartheta}_i^*$ of proof mass, the input angular rate Ω_z^*, the external disturbance $d_i^*(t^*)$, the damping term c_{ii}^0, the spring term k_{ii}^0, the damping coupling term $c_{ij}^0 (i \neq j)$, the spring coupling term $k_{ij}^0 (i \neq j)$, the nonlinear spring term k_{i3}^0, the control input u_i^*, the positive constant k_{di}, the unknown parameter variations $\Delta \boldsymbol{K}_1 \in \mathbb{R}^{2\times2}$ and $\Delta \boldsymbol{K}_2 \in \mathbb{R}^{2\times2}$, the dimensionless time $t = \omega_o t^*$, the reference frequency ω_o, the reference length ϑ_o, and $i = 1, 2, j = 1, 2$.

The external disturbance can be presented as $\boldsymbol{D} = \boldsymbol{D}^c + \boldsymbol{D}^h$, where $\boldsymbol{D}^c$ is the constant vibration and $\boldsymbol{D}^h$ is the harmonic signal. Define the lumped uncertainty as $\boldsymbol{R}(\boldsymbol{\vartheta}, \dot{\boldsymbol{\vartheta}}, t) = \boldsymbol{K}_d^{-1}(\boldsymbol{\mu} + \boldsymbol{K}_3 \boldsymbol{\vartheta}^3) + \boldsymbol{D}^c$. The dynamics (1) can be rewritten as

$$\ddot{\boldsymbol{\vartheta}} = \boldsymbol{K}_1^0 \dot{\boldsymbol{\vartheta}} + \boldsymbol{K}_2^0 \boldsymbol{\vartheta} + \boldsymbol{K}_d \boldsymbol{R} + \boldsymbol{K}_d \boldsymbol{D}^h + \boldsymbol{U}. \qquad (2)$$

HDOB-based SMC design for MEMS gyrosocpes. The harmonic disturbance is set as $\boldsymbol{D}^h = [\bar{\Lambda}_1 \sin(\varpi_1 t + \bar{\phi}_1), \bar{\Lambda}_2 \sin(\varpi_2 t + \bar{\phi}_2)]^{\mathrm{T}}$ with known frequencies ϖ_1, ϖ_2, unknown amplitudes $\bar{\Lambda}_1$, $\bar{\Lambda}_2$, and phases $\bar{\phi}_1$, $\bar{\phi}_2$. Considering

* Corresponding author (email: smileface.binxu@gmail.com)

the harmonic characteristic of $\boldsymbol{D}^h$, define $\boldsymbol{z}_1 = \boldsymbol{\vartheta}$, $\boldsymbol{z}_2 = \dot{\boldsymbol{\vartheta}}$, $\boldsymbol{z}_3 = \boldsymbol{D}^h$, $\boldsymbol{z}_4 = [\bar{\Lambda}_1 \cos(\varpi_1 t + \bar{\phi}_1), \bar{\Lambda}_2 \cos(\varpi_2 t + \bar{\phi}_2)]^{\mathrm{T}}$, and $\boldsymbol{z}_5 = \boldsymbol{R}$. The ESO of the dynamics (2) can be presented as

$$
\begin{cases}
\dot{\boldsymbol{z}}_1 = \boldsymbol{z}_2, \\
\dot{\boldsymbol{z}}_2 = \boldsymbol{K}_1^0 \boldsymbol{z}_2 + \boldsymbol{K}_2^0 \boldsymbol{z}_1 + \boldsymbol{U} + \boldsymbol{K}_d \boldsymbol{z}_3 + \boldsymbol{K}_d \boldsymbol{z}_5, \\
\dot{\boldsymbol{z}}_3 = \boldsymbol{W} \boldsymbol{z}_4, \\
\dot{\boldsymbol{z}}_4 = -\boldsymbol{W} \boldsymbol{z}_3, \\
\dot{\boldsymbol{z}}_5 = \boldsymbol{H},
\end{cases} \tag{3}
$$

where $\boldsymbol{W} = \mathrm{diag}(\varpi_1, \varpi_2)$ and $\boldsymbol{H} = \dot{\boldsymbol{R}}$.

Furthermore, the HDOB is designed as

$$
\begin{cases}
\dot{\hat{\boldsymbol{z}}}_1 = \hat{\boldsymbol{z}}_2 + \boldsymbol{\alpha}_1(\boldsymbol{z}_1 - \hat{\boldsymbol{z}}_1), \\
\dot{\hat{\boldsymbol{z}}}_2 = \boldsymbol{F} + \boldsymbol{U} + \boldsymbol{K}_d \hat{\boldsymbol{z}}_3 + \boldsymbol{K}_d \hat{\boldsymbol{z}}_5 + \boldsymbol{\alpha}_2(\boldsymbol{z}_1 - \hat{\boldsymbol{z}}_1), \\
\dot{\hat{\boldsymbol{z}}}_3 = \boldsymbol{W} \hat{\boldsymbol{z}}_4 + \boldsymbol{\alpha}_3(\boldsymbol{z}_1 - \hat{\boldsymbol{z}}_1), \\
\dot{\hat{\boldsymbol{z}}}_4 = -\boldsymbol{W} \hat{\boldsymbol{z}}_3 + \boldsymbol{\alpha}_4(\boldsymbol{z}_1 - \hat{\boldsymbol{z}}_1), \\
\dot{\hat{\boldsymbol{z}}}_5 = \boldsymbol{\alpha}_5(\boldsymbol{z}_1 - \hat{\boldsymbol{z}}_1),
\end{cases} \tag{4}
$$

where $\boldsymbol{F} = \boldsymbol{K}_1^0 \hat{\boldsymbol{z}}_2 + \boldsymbol{K}_2^0 \hat{\boldsymbol{z}}_1$, $\hat{\boldsymbol{z}}_\tau \in \mathbb{R}^{2 \times 1}$ ($\tau = 1, 2, \ldots, 5$) is the estimation of $\boldsymbol{z}_\tau$, and $\boldsymbol{\alpha}_\tau \in \mathbb{R}^{2 \times 2}$ is the positive definite observer gain.

Subtracting (4) from (3), it is obtained that

$$
\dot{\tilde{\boldsymbol{z}}} = \boldsymbol{A}_{\tilde{\boldsymbol{z}}} \tilde{\boldsymbol{z}} + \boldsymbol{B}_{\tilde{\boldsymbol{z}}} \boldsymbol{H}, \tag{5}
$$

where $\tilde{\boldsymbol{z}} = [\tilde{\boldsymbol{z}}_1^{\mathrm{T}}, \tilde{\boldsymbol{z}}_2^{\mathrm{T}}, \tilde{\boldsymbol{z}}_3^{\mathrm{T}}, \tilde{\boldsymbol{z}}_4^{\mathrm{T}}, \tilde{\boldsymbol{z}}_5^{\mathrm{T}}]^{\mathrm{T}} \in \mathbb{R}^{10 \times 1}$, $\tilde{\boldsymbol{z}}_\tau = \boldsymbol{z}_\tau - \hat{\boldsymbol{z}}_\tau$,

$$
\boldsymbol{A}_{\tilde{\boldsymbol{z}}} = \begin{bmatrix}
-\boldsymbol{\alpha}_1 & \boldsymbol{I} & \boldsymbol{0} & \boldsymbol{0} & \boldsymbol{0} \\
\boldsymbol{K}_2^0 - \boldsymbol{\alpha}_2 & \boldsymbol{K}_1^0 & \boldsymbol{K}_d & \boldsymbol{0} & \boldsymbol{K}_d \\
-\boldsymbol{\alpha}_3 & \boldsymbol{0} & \boldsymbol{0} & \boldsymbol{W} & \boldsymbol{0} \\
-\boldsymbol{\alpha}_4 & \boldsymbol{0} & -\boldsymbol{W} & \boldsymbol{0} & \boldsymbol{0} \\
-\boldsymbol{\alpha}_5 & \boldsymbol{0} & \boldsymbol{0} & \boldsymbol{0} & \boldsymbol{0}
\end{bmatrix},
$$

and $\boldsymbol{B}_{\tilde{\boldsymbol{z}}} = [\boldsymbol{0}, \boldsymbol{0}, \boldsymbol{0}, \boldsymbol{0}, \boldsymbol{I}]^{\mathrm{T}}$. $\boldsymbol{\alpha}_\tau$ is designed to force $\boldsymbol{A}_{\tilde{\boldsymbol{z}}}$ to satisfy Hurwitz condition.

The tracking error is defined as

$$
\boldsymbol{e}(t) = \boldsymbol{\vartheta} - \boldsymbol{\vartheta}_m, \tag{6}
$$

where $\boldsymbol{\vartheta}_m$ is the reference signal.

The sliding mode manifold is designed as

$$
\boldsymbol{s} = \boldsymbol{K}_s \boldsymbol{e}(t) + \dot{\boldsymbol{e}}(t), \tag{7}
$$

where $\boldsymbol{K}_s \in \mathbb{R}^{2 \times 2}$ satisfies Hurwitz condition.

Using the results of HDOB (4), the SMC is designed as

$$
\boldsymbol{U} = \ddot{\boldsymbol{\vartheta}}_m - \boldsymbol{K}_1^0 \dot{\boldsymbol{\vartheta}} - \boldsymbol{K}_2^0 \boldsymbol{\vartheta} - \boldsymbol{K}_d \hat{\boldsymbol{R}} - \boldsymbol{K}_d \hat{\boldsymbol{D}}^h - \boldsymbol{K}_s \dot{\boldsymbol{e}}(t) - \boldsymbol{K} \boldsymbol{s}, \tag{8}
$$

where $\boldsymbol{K} \in \mathbb{R}^{2 \times 2}$ is a positive definite matrix, $\hat{\boldsymbol{D}}^h = \hat{\boldsymbol{z}}_3$, $\hat{\boldsymbol{R}} = \hat{\boldsymbol{z}}_5$.

Theorem 1. Considering the dynamics described by (2), if the HDOB (4) and the controller (8) are designed, the tracking errors are bounded.

Remark 1. The proof of Theorem 1 can be obtained according to the analysis in [2]. The main difference is that in this paper, the HDOB is included and the related error dynamics analysis can be found in [5]. Thus the conclusion of the boundedness of the tracking errors can be guaranteed.

Remark 2. Define $\boldsymbol{\mu}_0(\boldsymbol{\vartheta}, \dot{\boldsymbol{\vartheta}}, t) = \boldsymbol{\mu} + \boldsymbol{K}_3 \boldsymbol{\vartheta}^3$. It is calculated that $\dot{\boldsymbol{\mu}}_0 = \frac{\partial \boldsymbol{\mu}_0}{\partial \boldsymbol{\vartheta}} \dot{\boldsymbol{\vartheta}} + \frac{\partial \boldsymbol{\mu}_0}{\partial \dot{\boldsymbol{\vartheta}}} \ddot{\boldsymbol{\vartheta}} + \frac{\partial \boldsymbol{\mu}_0}{\partial t}$. From [5], the partial derivative of time, and the partial differential polynomial of $\boldsymbol{\vartheta}, \dot{\boldsymbol{\vartheta}}$ are bounded. Thus there are positive constants $\bar{\mu}_1, \bar{\mu}_2$, such that $\|\boldsymbol{\mu}_0\| \leqslant \bar{\mu}_1$ and $\|\dot{\boldsymbol{\mu}}_0\| \leqslant \bar{\mu}_2$. For $\boldsymbol{R} = \boldsymbol{K}_d^{-1} \boldsymbol{\mu}_0 + \boldsymbol{D}^c$ and $\boldsymbol{H} = \dot{\boldsymbol{R}} = \boldsymbol{K}_d^{-1} \dot{\boldsymbol{\mu}}_0$, it is inferred that $\|\boldsymbol{R}\| \leqslant \frac{\bar{\mu}_1}{\lambda_{\mathrm{mind}}} + \bar{D}^c$ and $\|\boldsymbol{H}\| \leqslant \frac{\bar{\mu}_2}{\lambda_{\mathrm{mind}}}$, where λ_{mind} is the minimal eigenvalue of $\boldsymbol{K}_d$ and $\bar{D}^c = \|\boldsymbol{D}^c\|$.

Remark 3. To avoid impact damages, in practical applications, the external disturbances of MEMS gyroscopes are required to be bounded. Therefore, there are positive constants $\bar{D}_1$ and $\bar{D}_2$, such that $\|\boldsymbol{D}\| \leqslant \bar{D}_1$ and $\|\dot{\boldsymbol{D}}\| \leqslant \bar{D}_2$ exist.

HDOB-based GFTSMC design for MEMS gyrosocpes. The GFT sliding mode manifold [8] is defined as

$$
\boldsymbol{s} = \dot{\boldsymbol{e}}(t) + \boldsymbol{K}_{s1} \boldsymbol{e}(t) + \boldsymbol{K}_{s2} \boldsymbol{e}^{\frac{q}{p}}(t), \tag{9}
$$

where $\boldsymbol{K}_{s1} \in \mathbb{R}^{2 \times 2}$ and $\boldsymbol{K}_{s2} \in \mathbb{R}^{2 \times 2}$ satisfy Hurwitz condition, q and p are positive odd constants with $q < p$.

Using the results of HDOB (4), the GFTSMC is designed as follows:

$$
\boldsymbol{U} = \ddot{\boldsymbol{\vartheta}}_m - \boldsymbol{K}_1^0 \dot{\boldsymbol{\vartheta}} - \boldsymbol{K}_2^0 \boldsymbol{\vartheta} - \boldsymbol{K}_d \hat{\boldsymbol{R}} - \boldsymbol{K}_d \hat{\boldsymbol{D}}^h - \boldsymbol{F}_1 \boldsymbol{s}
$$
$$
- \boldsymbol{F}_2 \boldsymbol{s}^{\frac{q}{p}} - \left[\boldsymbol{K}_{s1} + \frac{q \boldsymbol{K}_{s2}}{p} \boldsymbol{e}^{\frac{q}{p}-1}(t) \right] \dot{\boldsymbol{e}}(t), \tag{10}
$$

where $\boldsymbol{F}_1 \in \mathbb{R}^{2 \times 2}$ and $\boldsymbol{F}_2 \in \mathbb{R}^{2 \times 2}$ are positive definite matrices, $\hat{\boldsymbol{D}}^h = \hat{\boldsymbol{z}}_3$, $\hat{\boldsymbol{R}} = \hat{\boldsymbol{z}}_5$.

Theorem 2. Considering the dynamics described by (2), if the HDOB (4) and the controller (10) are designed, the tracking errors are bounded and $\boldsymbol{s}$ converges to the bounded region in finite-time.

Remark 4. Different from Theorem 1, the finite-time convergence is guaranteed under the controller (10). The stability can be proved via the approach in [8].

Simulation. Mark the HDOB-based SMC as "HDOB-SMC", the HDOB-based GFTSMC as "HDOB-GFTSMC", and the DOB-based SMC as "DOB-SMC" with the controller $\boldsymbol{U} = \ddot{\boldsymbol{\vartheta}}_m - \boldsymbol{K}_1^0 \dot{\boldsymbol{\vartheta}} - \boldsymbol{K}_2^0 \boldsymbol{\vartheta} - \boldsymbol{K}_d \hat{\boldsymbol{\Upsilon}} - \boldsymbol{K}_s \dot{\boldsymbol{e}}(t) - \boldsymbol{K} \boldsymbol{s}$ and the DOB $\hat{\boldsymbol{\Upsilon}} = \boldsymbol{L}(\dot{\boldsymbol{\vartheta}} - \boldsymbol{\Psi})$, $\dot{\boldsymbol{\Psi}} = \boldsymbol{K}_1^0 \dot{\boldsymbol{\vartheta}} + \boldsymbol{K}_2^0 \boldsymbol{\vartheta} + \boldsymbol{K}_d \hat{\boldsymbol{\Upsilon}} + \boldsymbol{U}$.

The parameters of the MEMS gyroscope in [7] are used for simulation test. The dimensionless reference trajectory is set as $\boldsymbol{\vartheta}_m = [6.2 \sin(4.71t + \frac{\pi}{3}), 5 \cos(5.11t - \frac{\pi}{6})]^{\mathrm{T}}$. The control parameters are set as $\boldsymbol{K}_d = \mathrm{diag}(480, 600)$ and $\boldsymbol{K} = \mathrm{diag}(60, 66)$. For "DOB-SMC", $\boldsymbol{K}_s = \mathrm{diag}(60, 66)$, $\boldsymbol{L} = (0.4, 0.5)$. For "HDOB-SMC", $\boldsymbol{\alpha}_\tau = \mathrm{diag}(2000, 3000)$. For "HDOB-GFTSMC", $q = 15$, $p = 17$, $\boldsymbol{K}_{s1} = \mathrm{diag}(60, 66)$, $\boldsymbol{K}_{s2} = \mathrm{diag}(120, 110)$, $\boldsymbol{F}_1 = \mathrm{diag}(60, 66)$ and $\boldsymbol{F}_2 = \mathrm{diag}(100, 110)$. The harmonic disturbance is set as $\boldsymbol{D}^h = [\sin(5.6t), \sin(8t)]^{\mathrm{T}}$. The lumped uncertainty is set as $\boldsymbol{R} = [1 + 30 \sin(4.71t + \frac{7\pi}{9}), 1 + 35 \cos(5.11t + \frac{\pi}{3})]^{\mathrm{T}}$.

The simulation results are addressed in Figure 1. From the tracking errors shown in Figure 1(a), it is demonstrated that higher tracking accuracy is achieved under "HDOB-SMC" and "HDOB-GFTSMC". That is because, for multiple disturbance $\boldsymbol{\Upsilon} = \boldsymbol{R} + \boldsymbol{D}^h$, higher estimation accuracy is obtained under "HDOB-SMC" and "HDOB-GFTSMC" in Figure 1(b). Comparing the convergent rate of tracking errors, faster convergence is achieved under "HDOB-GFTSMC". In addition, due to the influence of $-q \boldsymbol{K}_{s2} \boldsymbol{e}^{\frac{q}{p}-1}(t) \dot{\boldsymbol{e}}(t)/p$ and $-\boldsymbol{F}_2 \boldsymbol{s}^{\frac{q}{p}}$ in the controller (10), it is observed from Figure 1(a) that better tracking performance is obtained under "HDOB-GFTSMC". The control inputs
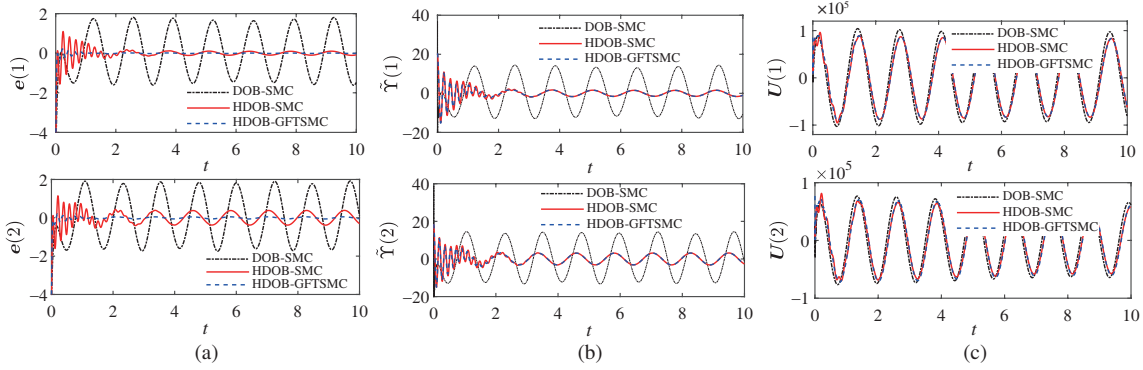
Figure 1   (Color online) Simulation results. (a) Tracking errors; (b) disturbances estimation errors; (c) control inputs.

are presented in Figure 1(c). Thus the above simulations confirm our expectation.

Conclusion. The HDOB-based SMC of MEMS gyroscopes is proposed in this study to deal with multiple disturbances, including the lumped uncertainty and the harmonic disturbance. Because the frequency information of harmonic disturbance is fully utilized by HDOB and GFTSMC is used, higher tracking accuracy and faster convergence are obtained under the proposed control scheme.

References

1   Park S, Horowitz R, Tan C W. Adaptive controller design of MEMS gyroscopes. In: Proceedings of Intelligent Transportation Systems, 2001. 496–501

2   Fei J T, Lu C. Adaptive sliding mode control of dynamic systems using double loop recurrent neural network structure. IEEE Trans Neural Netw Learn Syst, 2018, 29: 1275–1286

3   Fei J T, Feng Z L. Adaptive fuzzy super-twisting sliding mode control for microgyroscope. Complexity, 2019, 2019: 6942642

4   Zheng Q, Dong L L, Lee D H, et al. Active disturbance rejection control for MEMS gyroscopes. IEEE Trans Control Syst Technol, 2009, 17: 1432–1438

5   Hosseini-Pishrobat M, Keighobadi J. Robust output regulation of a triaxial MEMS gyroscope via nonlinear active disturbance rejection. Int J Robust Nonlinear Control, 2018, 28: 1830–1851

6   Rahmani M. MEMS gyroscope control using a novel compound robust control. ISA Trans, 2018, 72: 37–43

7   Xu B, Zhang R, Li S, et al. Composite neural learning-based nonsingular terminal sliding mode control of MEMS gyroscopes. IEEE Trans Neural Netw Learn Syst, 2020, 31: 1375–1386

8   Chen Z H, Yuan X H, Wu X T, et al. Global fast terminal sliding mode controller for hydraulic turbine regulating system with actuator dead zone. J Franklin Inst, 2019, 356: 8366–8387